

COHERENT SYNCHROTRON RADIATION AND WAKE FIELDS WITH DISCONTINUOUS GALERKIN TIME DOMAIN METHODS*

D. A. Bizzozero[†], H. De Gersem, E. Gjonaj

Institut für Theorie Elektromagnetischer Felder, TU Darmstadt, Germany

Abstract

Coherent synchrotron radiation (CSR) is an essential issue in modern accelerators. We propose a new method to examine CSR in the time domain using an unstructured Discontinuous Galerkin (DG) method. The method uses a 2D spatial discretization in the longitudinal and transverse coordinates (Z, X) with a Fourier series decomposition in the transverse coordinate Y and computes the fields modally. Additionally, by alignment of mesh element interfaces along a source reference orbit, DG methods can naturally handle discontinuous or thin sources in the transverse X direction. We present an overview of the method, illustrate it by calculating wake potentials in a model problem, and in a bunch compressor.

STATEMENT OF PROBLEM

In this work, we examine the generation of CSR by an ultra-relativistic electron bunch in a vacuum chamber of rectangular cross-section. We restrict motion of the bunch to a planar orbit with Cartesian coordinates (Z, X, Y) in the midplane $Y = 0$. Additionally, we only consider vacuum chambers with planar horizontal boundaries at $Y = \pm h/2$ where h is the height of the chamber. For our work, we consider only perfectly electrically conducting (PEC) boundary conditions on the chamber walls. An example of a chamber with a planar orbit is shown in Fig. 1, which models the bunch compressor DESY BC0.

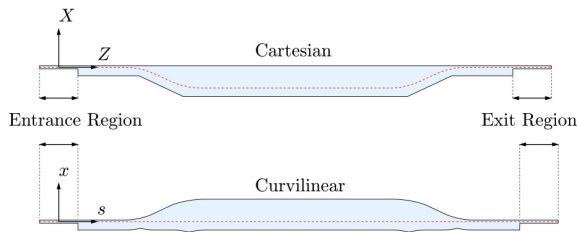


Figure 1: DESY BC0 vacuum chamber domain in (Z, X) (top) or (s, x) (bottom) coordinates with reference orbit (red dashed). The entrance region is the same in both systems.

To study CSR wake fields, we aim to time-evolve the Maxwell field equations for \mathbf{E} and \mathbf{H} inside the chamber:

$$\frac{\partial \mathbf{E}}{\partial \tau} = Z_0 \nabla \times \mathbf{H} - Z_0 \mathbf{j}, \quad \frac{\partial \mathbf{H}}{\partial \tau} = -\frac{1}{Z_0} \nabla \times \mathbf{E}, \quad (1)$$

* Work supported by DESY.

[†] bizzozero@temf.tu-darmstadt.de

where $\tau = ct$, with speed of light c , vacuum impedance Z_0 , and current density \mathbf{j} .

Given a smooth reference orbit parametrized by arc length $\mathbf{R}_r(s) = (Z_r(s), X_r(s), 0)$, we transform the (Z, X, Y) coordinate system to a curvilinear system (s, x, y) with the inverse transformation of:

$$\begin{aligned} Z(s, x) &= Z_r(s) - xX_r'(s), \\ X(s, x) &= X_r(s) + xZ_r'(s), \end{aligned} \quad (2)$$

with the coordinate $Y = y$ unchanged. It is also useful to define the signed curvature $\kappa(s) = Z_r''(s)X_r'(s) - Z_r'(s)X_r''(s)$ and length scale factor $\eta(s, x) = 1 + x\kappa(s)$. In the (s, x, y) coordinate system, the reference orbit is the straight line $(x, y) = (0, 0)$. Furthermore, this coordinate mapping is well-defined if $\eta > 0$ throughout the domain; where the transformation is unique.

In the (s, x, y) coordinate frame, we assume a current density of the form: $\mathbf{j} = (qc\lambda(s - \tau)\delta(x)G(y), 0, 0)$ with Gaussian longitudinal and transverse distributions λ and G , and a Dirac distribution in the x -coordinate. We choose σ_y , the RMS width of G , such that $\sigma_y \ll h$ so that $G(\pm h/2) = 0$ to machine precision. Similarly, we choose σ_s , the RMS bunch length, such that the bunch is compactly supported in the entrance region to machine precision.

We next use the parallel plate geometry of $y = \pm h/2$ to introduce a Fourier decomposition in y :

$$\begin{aligned} f(s, x, y, \tau) &= \sum_{p=1}^{\infty} f_p(s, x, \tau) \phi(\alpha_p(y + h/2)), \\ f_p(s, x, \tau) &= \frac{2}{h} \int_{-h/2}^{h/2} f(s, x, y, \tau) \phi(\alpha_p(y + h/2)) dy, \end{aligned} \quad (3)$$

with $\alpha_p = \pi p/h$, f representing $E_s, E_x, E_y, H_s, H_x, H_y$ or G , and $\phi(\cdot)$ is $\sin(\cdot)$ for E_s, E_x, H_y, G and $\cos(\cdot)$ for E_y, H_s, H_x . If the initial fields and $G(y)$ is symmetric about $y = 0$, then even p modes for all fields vanish. We denote the Fourier series modes with the subscript p .

Due to numerical difficulties in handling the singularity at $x = 0$ in the current \mathbf{j} term on the right-hand-side of (1), we apply an additional transformation on the H_{yp} field component: $\tilde{H}_{yp} = H_{yp} - qcG_p\lambda(s - \tau)\Theta(x)$ where $\Theta(x)$ is the Heaviside function. Additional transformations can be made to transform the source to arbitrary degree of smoothness [1]; however, for a DG method with element edges which align along the discontinuity, this is not required.

Applying the curvilinear coordinate transformation in (2), the Fourier series decomposition in (3), and the transforma-

tion for H_{yp} , to (1) yields:

$$\frac{1}{Z_0} \frac{\partial E_{sp}}{\partial \tau} = \frac{\partial \tilde{H}_{yp}}{\partial x} + \alpha_p H_{xp}, \quad (4a)$$

$$\frac{1}{Z_0} \frac{\partial E_{xp}}{\partial \tau} = -\alpha_p H_{sp} - \frac{1}{\eta} \frac{\partial \tilde{H}_{yp}}{\partial s} + S_E, \quad (4b)$$

$$\frac{1}{Z_0} \frac{\partial E_{yp}}{\partial \tau} = \frac{1}{\eta} \frac{\partial H_{xp}}{\partial s} - \frac{\partial H_{sp}}{\partial x} - \frac{\kappa}{\eta} H_{sp}, \quad (4c)$$

$$Z_0 \frac{\partial H_{sp}}{\partial \tau} = \alpha_p E_{xp} - \frac{\partial E_{yp}}{\partial x}, \quad (4d)$$

$$Z_0 \frac{\partial H_{xp}}{\partial \tau} = \frac{1}{\eta} \frac{\partial E_{yp}}{\partial s} - \alpha_p E_{sp}, \quad (4e)$$

$$Z_0 \frac{\partial \tilde{H}_{yp}}{\partial \tau} = \frac{\partial E_{sp}}{\partial x} + \frac{\kappa}{\eta} E_{sp} - \frac{1}{\eta} \frac{\partial E_{xp}}{\partial s} + S_H, \quad (4f)$$

where the source terms $S_E = -qcG_p \lambda'(s - \tau) \Theta(x) / \eta(s, x)$ and $S_H = qZ_0 c G_p \lambda'(s - \tau) \Theta(x)$ arise from \mathbf{j} after the H_{yp} transformation.

To initialize the time-evolution of the system in (4) we consider all fields inside the vacuum chamber to be zero initially except for the entrance region. In this region, where the reference orbit is a straight line in (Z, X, Y) with $\kappa = 0$, $\eta = 1$; we derive a solution for a centered beam about $x = 0$ with total width $2d$ satisfying the PEC boundary conditions:

$$\begin{aligned} E_{sp0} &= 0, & H_{sp0} &= 0, \\ E_{xp0} &= -qZ_0 c G_p \lambda(s) \Phi(x), & H_{xp0} &= -E_{yp0} / Z_0, \\ E_{yp0} &= -qcZ_0 G_p \lambda(s) \Psi(x), & H_{yp0} &= E_{xp0} / Z_0, \end{aligned} \quad (5)$$

$$\Phi(x) = \frac{\sinh(\alpha_p d)}{\sinh(2\alpha_p d)} \cosh(\alpha_p(x - d)) - \cosh(\alpha_p x) \Theta(x),$$

$$\Psi(x) = \frac{\sinh(\alpha_p d)}{\sinh(2\alpha_p d)} \sinh(\alpha_p(x - d)) - \sinh(\alpha_p x) \Theta(x).$$

Lastly, the open port boundaries in the s -coordinate are also set with PEC conditions since the simulation is set to halt once the electron bunch reaches midway into the exit region of the chamber. If longer wake field simulations are desired, this exit region may be extended with little additional computational effort since the cross-sectional width is small. An earlier version of this method was presented in [2] and applied to an accelerator structure at the Canadian Light Source, Saskatoon, Canada [3].

DISCONTINUOUS GALERKIN METHOD

In this section we outline the DG scheme used for our time-evolution of (4). Our approach follows the nodal DG foundation given in [4]. To begin, we partition the vacuum chamber domain in (s, x) into K triangular elements, with curved elements along the boundary as needed. Additionally, we impose that the reference orbit $x = 0$ lie strictly along interfaces of elements and not bisect any element. For a given element D^k , for $k \in \{1, \dots, K\}$, we approximate each field by a Lagrange polynomial of N th order denoted by

$\ell_j^k(s, x)$ with $N_p = (N + 1)(N + 2)/2$ nodes: (s_i^k, x_i^k) where $\ell_j^k(s_i^k, x_i^k) = \delta_{ij}$, for $i, j \in \{1, \dots, N_p\}$. For a field component u on element D^k , its polynomial approximation is given by:

$$u^k(s, x, \tau) = \sum_{i=1}^{N_p} u_i^k(\tau) \ell_i^k(s, x). \quad (6)$$

We next construct residuals \mathcal{R}^k for each of the fields u^k from (4) which each have the form:

$$\mathcal{R}^k(s, x, \tau) = \frac{\partial u^k}{\partial \tau} - a \frac{\partial v^k}{\partial s} - b \frac{\partial w^k}{\partial x} - cw^k - f. \quad (7)$$

For example, for equation (4c): $u = E_{yp}$, $v = \tilde{H}_{xp}$, $w = H_{sp}$, $a = Z_0/\eta$, $b = -Z_0$, $c = -Z_0\kappa/\eta$, and $f = 0$. For a Galerkin scheme, we require the residuals to be orthogonal to the same polynomial space spanned by ℓ_j^k on the element. However, a numerical flux must be introduced to couple the elements together along their edges. This flux term is derived by first integrating \mathcal{R}^k with each test function ℓ_j^k over the element D^k by parts, then adjusting the boundary term to incorporate information from elements neighboring D^k , and lastly integrating by parts back to arrive at:

$$\begin{aligned} \int_{D^k} \mathcal{R}^k(s, x, \tau) \ell_j^k(s, x) ds dx &= \\ - \int_{\partial D^k} \mathbf{n} \cdot [av^k - (av)^*, bw^k - (bw)^*] \ell_j^k(s, x) dl, \end{aligned} \quad (8)$$

where $\mathbf{n} = [n_s, n_x]$ denotes the outward normal unit vector along the boundary of D^k , and $(\cdot)^*$ denotes the numerical flux: a single-valued function depending on interior and exterior values along the interface. We choose an upwind flux for our hyperbolic system of equations (4).

In implementing the DG scheme outlined above, we build the discrete $N_p \times N_p$ matrix operators: \mathcal{M}^k , \mathcal{D}_s^k , \mathcal{D}_x^k so that:

$$\begin{aligned} \mathcal{D}_s^k &= [\mathcal{M}^k]^{-1} \mathcal{S}_s^k, & [\mathcal{M}^k]_{ij} &= \int_{D^k} \ell_i^k(s, x) \ell_j^k(s, x) ds dx, \\ \mathcal{D}_x^k &= [\mathcal{M}^k]^{-1} \mathcal{S}_x^k, & [\mathcal{S}_{s;x}^k]_{ij} &= \int_{D^k} \ell_i^k(s, x) \frac{\partial \ell_j^k(s, x)}{\partial s; x} ds dx. \end{aligned}$$

Combining these operators with the residual formulation from (7) with (8) yields N_p semi-discrete equations for each field. In the example for equation (4c), these semi-discrete equations are (with the superscript k suppressed):

$$\begin{aligned} \frac{1}{Z_0} \frac{d\bar{E}_{yp}}{d\tau} &= \frac{1}{\bar{\eta}} \circ (\mathcal{D}_s \bar{H}_{xp}) - \mathcal{D}_x \bar{H}_{sp} - \frac{\bar{\kappa}}{\bar{\eta}} \circ \bar{H}_{sp} - \\ \frac{1}{2} (J\mathcal{M})^{-1} &\left[\frac{\bar{n}_s}{\bar{\eta}} \circ \llbracket \underline{H}_{xp} \rrbracket - \bar{n}_x \circ \llbracket \underline{H}_{sp} \rrbracket + \frac{1}{Z_0} \llbracket \underline{E}_{yp} \rrbracket \right], \end{aligned} \quad (9)$$

where an upper bar $\bar{\cdot}$ denotes the vector of N_p nodal weights on element k , a lower bar $\underline{\cdot}$ denotes the vector of $3(N + 1)$ boundary nodes for each element (shared with a neighboring element), \circ denotes a Hadamard (element-wise) product, and $\llbracket u \rrbracket = u_{\text{int}} - u_{\text{ext}}$ denotes the jump in field values along the

interface. The surface integral operator $(JM)^{-1}$ is of size $N_p \times 3(N + 1)$. A thorough derivation of (9) is given in [2] with DG constructions detailed in [4].

The PEC boundary conditions are imposed by setting the jumps for the tangential component of \mathbf{E} to twice its value on the boundary such that the mean vanishes. In the example for (4c), this is imposed by setting $[[E_{yp}]] = 2E_{yp}$ along the boundary, since the y unit-vector is orthogonal to the domain. Although, analytic expressions for the initial fields (5) are known, we initialize the DG fields with a DG Helmholtz equation solver outlined in [4] to reduce parasitic charge remaining in the entrance region.

With equations similar to (9) for (4a)-(4f), and combining all K elements, we obtain a system of $6N_p K$ equations. We evolve these equations in τ with a fourth-order low-storage explicit Runge-Kutta scheme [5].

SIMULATIONS AND RESULTS

We present simulation results for computing the longitudinal wake field by integrating E_s along the reference orbit. We define the longitudinal wake function on the orbit by:

$$\begin{aligned} w_s(z) &= \frac{-1}{q} \int_0^T E_s(\tau - z, 0, 0, \tau) d\tau \\ &= \frac{-1}{q} \sum_{p=1}^{p_{\max}} \sin\left(\frac{\pi p}{2}\right) \int_0^T E_{sp}(\tau - z, 0, \tau) d\tau. \end{aligned} \quad (10)$$

We denote z as the distance with respect to the center of the bunch along the reference orbit, not the Cartesian coordinate Z . Evaluation of E_{sp} is done while time-stepping (4a) by averaging the field along $x = 0$ using the elements' DG N th-order polynomial representation as in (6). We set T/c to be time when the bunch is midway into the exit region.

In our first test, we consider a straight orbit such that $(s, x) = (Z, X)$ where the bunch passes through a rectangular taper. While no CSR is generated, the narrowing width of the chamber generates a longitudinal wake in Fig. 2. This test is used to compare wake fields to CST Particle Studio™ [6] which cannot prescribe curved particle trajectories.

In our second test, we use the full DESY BC0 geometry as shown in Fig. 1. In Fig. 3, we plot the longitudinal wake wake generated by CSR and the geometry after the bunch travels along the chicane orbit comprised of straights and arcs of circles with constant curvature $\kappa = 1 \text{ m}^{-1}$.

CONCLUSION AND FUTURE WORK

In this study, we computed CSR generated in a bunch compressor vacuum chamber using DG finite elements in the time domain. While our approach works well for bunches of small transverse dimensions, modeling very thin longitudinal distributions becomes exceedingly costly as the DG mesh must resolve features smaller than σ_s .

Our next application of this DG method will study the evolution of particle distributions by importing wake potentials with ASTRA [7]. We also will compare our results to paraxial frequency-domain methods [8].

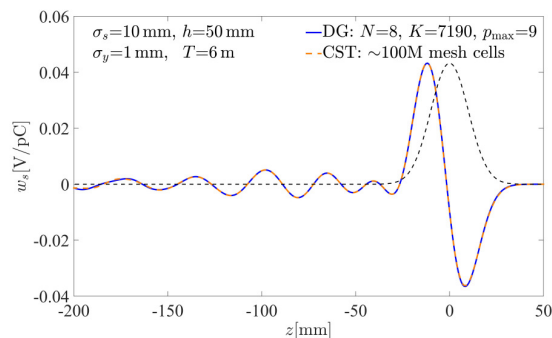


Figure 2: Wake function $w_s(z)$ for the test tapered chamber with a comparison result from CST Particle Studio™ with the direct wake solver. The thin dashed line shows the bunch profile $\lambda(z)$ scaled to $w_s(z)$.

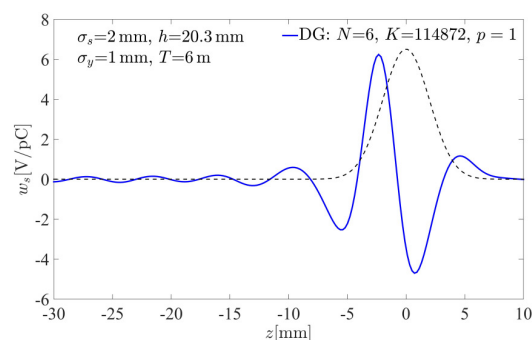


Figure 3: Wake function $w_s(z)$ shown using only the $p = 1$ mode for the DESY BC0 vacuum chamber. The thin dashed line shows the bunch profile $\lambda(z)$ scaled to $w_s(z)$.

REFERENCES

- [1] R. L. Warnock and D. A. Bizzozero, "Efficient Computation of Coherent Synchrotron Radiation in a Rectangular Chamber", *Phys. Rev. Accel. Beams* **19**, 090705, 2016.
- [2] D. A. Bizzozero, *Studies of Coherent Synchrotron Radiation with the Discontinuous Galerkin Method*, Ph.D. Dissertation, Applied Math, University of New Mexico, 2015.
- [3] B. E. Billinghamurst et al., "Observation of Wakefields and Resonances in Coherent Synchrotron Radiation", *Phys. Rev. Lett.* **114**, 204801, 2015.
- [4] J. Hesthaven and T. Warburton, *Nodal Discontinuous Galerkin Methods* New York: Springer, 2008.
- [5] J. C. Butcher, *The Numerical Analysis of Ordinary Differential Equations: Runge-Kutta and General Linear Methods*, New York: Wiley & Sons, 2003.
- [6] CST AG (2016), Bad Nauheimer Str. 19, 64289 Darmstadt, Germany.
- [7] M. Dohlus, K. Flottmann, and C. Henning, "Fast Particle Tracking With Wake Fields", DESY 12-012, arXiv:1201.5270, 2012.
- [8] D. Zhou, K. Ohmi, K. Oide, L. Zang, and G. Stupakov, "Calculation of Coherent Synchrotron Radiation Impedance for a Beam Moving in a Curved Trajectory", *Jpn. J. Appl. Phys.* **51**, 016401, 2012.